

# HEAT AND MASS TRANSFER MODEL IN WOOD CHIP DRYING

*Maria Eugênia de Paiva Souza*

Chemical Engineer  
Dep. de Mecânica e Eletricidade  
Instituto de Pesquisas Tecnológicas (IPT)  
P.O. Box 7141, 01064-970  
São Paulo, S.P., Brazil

and

*Silvia Azucena Nebra*

Associate Professor  
Dep. de Energia (DE—FEM), Univ. Estadual de Campinas (UNICAMP)  
P.O. Box 6122, 13083-970  
Campinas, S.P., Brazil

(Received October 1998)

## ABSTRACT

A model of simultaneous transport of heat and mass in a hygroscopic capillary porous medium was developed and applied to the drying of wood. Water is considered to be present in three forms—free water, bound water, and vapor—which remain in local equilibrium. It is assumed that the heat and mass transport mechanisms are: capillarity of free water, diffusion of vapor due to the concentration gradient, and diffusion of bound water due to the gradient of chemical potential between the water molecules. The constants of the phenomenological coefficients were adjusted. Finally, the drying process in wood chips was simulated in a unidimensional mesh. The results were compared with experimental data on drying kinetics obtained from the literature. Concentration profiles are shown, and the weight of each of the mechanisms present in the drying phenomenon is shown in graphic form and discussed.

*Keywords:* Capillarity, chips, diffusion of vapor, diffusion of bound water.

## INTRODUCTION

Interest in the study of the drying of wood chips derives from the fact that they are used as fuel in the boilers of the cellulose and paper industry. Before being fed, they are dried by effluent gases from the boiler itself, so an appropriate drying process is essential if the goal of saving energy is pursued.

The objective of this work is the development of a model for the drying process of a hygroscopic capillary porous medium focusing on the case of wood chips; however, the model can be extended to other cases. The chips have a prismatic form and a thickness that is considerably smaller than the other two dimensions; the phenomena of heat and mass transfer were considered to occur preferentially in the shorter dimensional direction, which is normal to the planes of bigger area (Fig. 1).

Simultaneous heat and mass transfer and equilibrium conditions between the phases were assumed; physical and transport properties found in the literature were used. The equations system obtained was numerically solved, and the results of the simulation are presented and compared with experimental data from the literature. The moisture content and temperature profiles are presented and discussed.

## DRYING MODEL

The drying phenomenon was treated as a simultaneous process of heat and mass transfer that occurs inside and outside of the chip. Three states of water were considered: free water, bound water, and vapor. It was assumed that all three phases were in thermodynamic equilibrium at the local temperature. There-

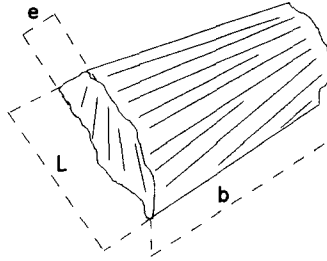


FIG. 1. Chip geometry.

fore, the evaporative flux was determined locally from the heat and mass fluxes, which were calculated with the variables constrained by the equilibrium conditions.

Each of the states of the water was submitted to one of the following transport mechanisms:

- 1) migration of free water by total pressure gradient flow as estimated by Darcy's law;
- 2) transfer of bound water by diffusion due to the chemical potential gradient;
- 3) migration of vapor by diffusion due to the partial pressure gradient of water vapor. The assumptions adopted were:
- 4) The drying phenomenon inside the chip was considered unidimensional.
- 5) There were no shrinkage effects, and the bound water was part of the solids phase.
- 6) Local thermodynamic equilibrium occurred at each point of the sample. Bound water and vapor are in equilibrium according to the sorption isotherms for wood, and they remain in a saturated state while free water is present.
- 7) The drying process occurred due to the internal and external evaporation, the diffusion of bound water and vapor, and the capillarity of free water.
- 8) The high permeability did not permit an increase in internal pressure, which remains the same as ambient pressure. Thus there was no internal convective flux of vapor (because there was no total pressure gradient).
- 9) The evaporation of bound water began inside the particle only when free water was no longer present.

### Differential equations of conservation

Free and bound water were considered to be migrating together; the balance of the liquid phase is:

$$\frac{\partial(\rho_s C_{bf})}{\partial t} = -\frac{\partial J_{bf}}{\partial x} - R_{\text{evap}} \quad (1)$$

where

$$C_{bf} = C_f + C_b \quad \text{and} \quad \rho_s = \rho_c(1 - \epsilon_s).$$

The symbol  $\rho_c$  is the cell-wall density equal to 1,500 kg/m<sup>3</sup>.

$$\text{vapor phase:} \quad \frac{\partial(\rho_s C_v)}{\partial t} = -\frac{\partial J_v}{\partial x} + R_{\text{evap}} \quad (2)$$

$$\text{energy:} \quad \rho_{sw} c_{psw} \frac{\partial T}{\partial t} = -\frac{\partial J_q}{\partial x} - R_{\text{evap}} \Delta H \quad (3)$$

where

$$\rho_{sw} = \rho_s(1 + C_{bf})$$

The symbol  $\Delta H$  is equal to the vaporization enthalpy of liquid water while free water is present; otherwise,  $\Delta H$  is equal to the vaporization enthalpy of bound water (vaporization enthalpy of liquid water plus desorption enthalpy of bound water).

In Eq. (3), the terms referring to convective heat flux due to liquid phase diffusion and flux due to vapor phase diffusion were disregarded (the term referring to the convective transport of energy due to mass diffusion is negligible compared to the conductive term (Souza 1994)).

### Equilibrium correlations

Equations (1), (2), and (3) form a partial differential equations system, in space and time, with four independent variables:  $C_{bf}$ ,  $C_v$ ,  $T$ ,  $R_{\text{evap}}$ . For this system to become determinate, another equation is necessary. It is given by the local equilibrium correlations for free and bound water in equilibrium with saturated vapor, and when free water is no longer present, bound water and vapor obey the sorption isotherms.

When free water is present, the concentration of vapor in the wood is

$$C_v^{\text{sat}} = \rho_v^{\text{sat}} \frac{\epsilon}{\rho_s}$$

where

$$\rho_v^{\text{sat}} = \frac{M_v p_v^{\text{sat}}}{RT},$$

and using the correlation given by Stanish et al. (1986) to calculate the density of saturated vapor,  $\rho_v^{\text{sat}}$ , for a temperature interval from 300 to 500 K with an error of 1%

$$C_v^{\text{sat}} = \frac{\epsilon}{\rho_s} \exp[-46.490 + 0.26179(T) - 5.0104 \times 10^{-4}(T)^2 + 3.4712 \times 10^{-7}(T)^3] \quad (4)$$

where

$$\epsilon = \epsilon_s - \frac{\rho_s}{\rho_f} C_f$$

When only bound water in equilibrium with water vapor is inside the solid, moisture content  $C_v$  is given by the following isotherms of Simpson and Rosen (1981), also used by Stanish, et al. (1986):

$$C_v = C_v^{\text{sat}} \left\{ Z_1 + \left[ (Z_1)^2 + \frac{1}{a_1(a_2)^2} \right]^{1/2} \right\} \quad (5)$$

where

$$Z_1 = \frac{[1 - Z_2]}{2a_2} - \frac{[1 + Z_2]}{2a_1 a_2} \quad Z_2 = \frac{18}{WC_b}$$

$$a_1 = -45.70 + 0.3216(T) - 5.012 \times 10^{-4}(T)^2$$

$$a_2 = 0.1722 + 4.732 \times 10^{-3}(T) - 5.553 \times 10^{-6}(T)^2$$

$$w = 1,417 - 9.430(T) + 1.853 \times 10^{-2}(T)^2.$$

#### Transport mechanisms

In the case of the *flux of liquid water*, it was assumed that free and bound water migrate jointly, so the liquid flux will be proportional to the liquid phase concentration, as follows:

$$J_{\text{bf}} = -(\rho_s D_{\text{bf}}) \frac{\partial C_{\text{bf}}}{\partial x} \quad (6)$$

where

$$D_{\text{bf}} = \left( \frac{C_b}{C_{\text{bf}}} \right) D_b + \left( \frac{C_f}{C_{\text{bf}}} \right) D_f. \quad (7)$$

Hence, a mean diffusion coefficient, obtained from the effective diffusivities, was used.

The effective diffusivities of free and bound water were obtained from the individual mechanisms of both of the forms, as will be explained below.

The free water flux is based on Darcy's law for porous media, so it is proportional to the total pressure gradient of the liquid. The total pressure of the liquid is equal to the pressure of the gas phase minus the capillarity pressure at the gas liquid interface, as follows:

$$J_f = -\rho_f \left( \frac{k_f}{\eta_f} \right) \frac{\partial}{\partial x} (P - P_c). \quad (8)$$

Spolek and Plumb (1981) measured the capillarity pressure of *Pinus* and suggested the correlation:

$$P_c = 10,000(\rho_s C_f / \epsilon_s \rho_f)^{-0.61} \quad (9)$$

Substituting the capillarity pressure given by Eq. (9) in Eq. (8), disregarding the total pressure gradient inside the particle, and assuming that the flux in Eq. (8) can be described by Fick's law, we get:

$$-D_f \frac{\partial(\rho_s C_f)}{\partial x} = 10^4 \rho_f \left( \frac{k_f}{\eta_f} \right) \frac{\partial}{\partial x} \left( \frac{\rho_s C_f}{\rho_f \epsilon_s} \right)^{-0.61} \quad (10)$$

which permits the calculation of effective diffusivity of the free water, that varies with concentration and local temperature in the following way:

$$D_f = 6.1 \times 10^3 \left( \frac{k_f}{\eta_f} \right) \epsilon_s^{0.61} \left( \frac{\rho_s C_f}{\rho_f} \right)^{-1.61} \quad (11)$$

It was assumed that the *flux of bound water* is proportional to the chemical potential gradient of the water bound to the solid, and at the volume fraction occupied by the solid:

$$J_b = -D_b^*(1 - \epsilon_s) \frac{\partial \mu_b}{\partial x} \quad (12)$$

Due to the assumption of local thermodynamic equilibrium, the chemical potential of the water adsorbed inside the solid is equal to the chemical potential of the water vapor in the interstitial spaces between cells, as follows:

$$\mu_b = \mu_v$$

For gases, Gibbs-Duhem's law permits us to write:

$$M_v \cdot \partial \mu_v = -S_v \partial T + V \cdot \partial p_v$$

Then, the bound water flux can be expressed in terms of the following vapor phase properties:

$$J_b = -D_b^*(1 - \epsilon_s) \left[ -\left( \frac{S_v}{M_v} \right) \frac{\partial T}{\partial x} + \left( \frac{\epsilon}{\rho_s C_v} \right) \frac{\partial p_v}{\partial x} \right] \quad (13)$$

Making the  $J_b$  in Fick's law equal to expression (13), we have

$$D_b = \frac{D_b^*(1 - \epsilon_s)}{\rho_s} \left[ -\left( \frac{S_v}{M_v} \right) \left( \frac{\partial T}{\partial C_b} \right)_{p_v} + \left( \frac{\epsilon}{\rho_s C_v} \right) \left( \frac{\partial p_v}{\partial C_v} \right)_T \right] \quad (14)$$

where the vapor partial pressure is correlated with the vapor concentration by the law of ideal gases (see Eq. (4)) and the partial derivatives are obtained from the equilibrium isotherms (see Eq. (5) (Souza 1994)).

The *transport mechanism of water vapor*, inside the solid, was assumed to be diffusion, so

$$J_v = -\left( \frac{\rho_s D_v}{\epsilon} \right) \frac{\partial C_v}{\partial x} \quad (15)$$

where

$$D_v = \alpha D_{rp} = \alpha D_{a,v} \epsilon^2$$

It was assumed that effective diffusivity depends on random diffusivity, with a correction factor due to possibly obstructed pores inside the wood;  $D_{a,v}$  is the diffusivity of the water

vapor in the air and  $\alpha$  is a factor that corrects the effect of possibly obstructed pores (Kayihan 1982).

The only mechanism adopted for *heat transfer* was conduction:

$$J_q = -k \frac{\partial T}{\partial x} \quad (16)$$

#### Boundary conditions

Each of the differential equations, (1), (2), and (3), requires one initial and two boundary conditions.

The initial temperatures and vapor and bound water concentrations need to obey the thermodynamic equilibrium correlations. Therefore, if free water is present, these concentrations are calculated by Eq. (4), with a relative moisture content of the air equal to 100%, and if free water is absent, Eq. (5) is used.

The first boundary condition for each of the differential balance equations is given by the heat and mass convection on the limit surface of the chips, and the second is given by the symmetry conditions.

In  $x = 0$  (chip surface),

$$J_v = k_m(p_{vo} - p_{vg}) \quad J_q = h_m(T_g - T_o) \\ J_{bf} = 0. \quad (17)$$

In  $x = e/2$  (chip center),

$$-D_{bf} \frac{\partial(\rho_s C_{bf})}{\partial x} \Big|_{x=e/2} = -D_v \frac{\partial(\rho_s C_v)}{\partial x} \Big|_{x=e/2} = 0 \quad \text{and} \\ -k \frac{\partial T}{\partial x} \Big|_{x=e/2} = 0 \quad (18)$$

#### Thermodynamic relations and physical and transport properties

Treating the water vapor as an ideal gas, Moore calculated a reference value of 187 J/mol K, corresponding to 298.15 K and 101.325 KPa, and obtained the correlation below for other states.

$$S_v = 187.0 + 35.1 \ln\left(\frac{T}{298.15}\right) - 8.314 \ln\left(\frac{p_v}{101,325}\right) \quad [\text{J}/(\text{mol K})] \quad (19)$$

The vaporization enthalpy of free water was taken from the Keenan's Steam Tables, (Stanish et al. 1986), as follows:

$$\Delta H = \Delta H_f = 2.792 \times 10^6 - 160(T) - 3.43(T)^2 \quad [\text{J}/\text{kg}] \quad (20)$$

The vaporization enthalpy of bound water is given by Stanish et al. (1986), as:

$$\Delta H = \Delta H_b = \Delta H_f \left[ 1 + 0.4 \left( 1 - 2 \frac{C_b}{C_{fsp}} + \left( \frac{C_b}{C_{fsp}} \right)^2 \right) \right] \quad [\text{J}/\text{kg}] \quad (21)$$

where  $C_{fsp}$ , given by Eq. (5), is the concentration of bound water in equilibrium with the saturated vapor for 100% relative moisture content of the air.

The thermal conductivity of the humid wood was taken from the Wood Handbook (1974), with modifications by Kayihan (1982), as follows:

$$k = 1.5(1 - \epsilon_s)(0.20 + 0.50X) + 0.024 \quad [\text{J}/(\text{m s K})] \quad (22)$$

where  $X = C_v + C_{bf}$  is the moisture content (dry base) of the solid.

The following specific heat of the humid wood was given by Siau (1971), in Kayihan (1982):

$$c_{psw} = \frac{X + 0.324}{1 + X} (4,184) \quad [\text{J}/(\text{kg K})] \quad (23)$$

The diffusivity of the water vapor in the air, gotten from Kanury (1975), in Kayihan (1982), is:

$$D_{a,v} = 1.2 \times 10^{-9}(T)^{1.75} \quad [\text{m}^2/\text{s}] \quad (24)$$

The density of the liquid water (Stanish et al. 1986) is:

$$\rho_f = 1,157.8 - 0.5362(T) \quad [\text{kg}/\text{m}^3] \quad (25)$$

The viscosity of the liquid water, given by Weast (1974), in Stanish et al. (1986):

$$\log_{10}(\eta_f) = -13.73 + \frac{1,828}{T} + 1.966 \times 10^{-2}(T) - 1.466 \times 10^{-5}(T)^2 \quad [\text{kg}/(\text{m s})] \quad (26)$$

The convective heat transfer coefficient at the external boundary layer, in this case, was adjusted using the experimental drying curve.

For the mass transfer coefficient, the analogy of Chilton-Colburn was used, according to the driving force considered in Eq. (17) and considering that the total pressure is constant, the coefficient was deduced from Bird et al. 1960:

$$k_m = \frac{h_m M_v \left( \frac{Pr}{Sc} \right)^{2/3}}{P \tilde{c}_{pg}} \quad [\text{kg}/\text{m}^2 \text{ s Pa}] \quad (27)$$

The wood-water effective permeability was given by Tesoro et al. (1974) as:

$$k_f = \begin{cases} 0 & \text{if } \left( \frac{\rho_s C_f}{\epsilon_s \rho_f} \right) \leq S_{ir} \\ k_f^\phi \left( 1 - \cos \frac{\pi}{2} \left( \frac{(\rho_s C_f / \epsilon_s \rho_f) - S_{ir}}{1 - S_{ir}} \right) \right) & \text{if } \left( \frac{\rho_s C_f}{\epsilon_s \rho_f} \right) > S_{ir} \end{cases} \quad (28)$$

The value of  $S_{ir}$ , "irreducible saturation," is where the column of liquid water breaks into the pores; above this value permeability increases as relative saturation increases.

#### NUMERICAL METHOD

The numerical solution of the equations system proposed was conducted by transforming each differential partial equation in time and space into  $(N+1)$  algebraic equations by the discretization of time, and particle thickness

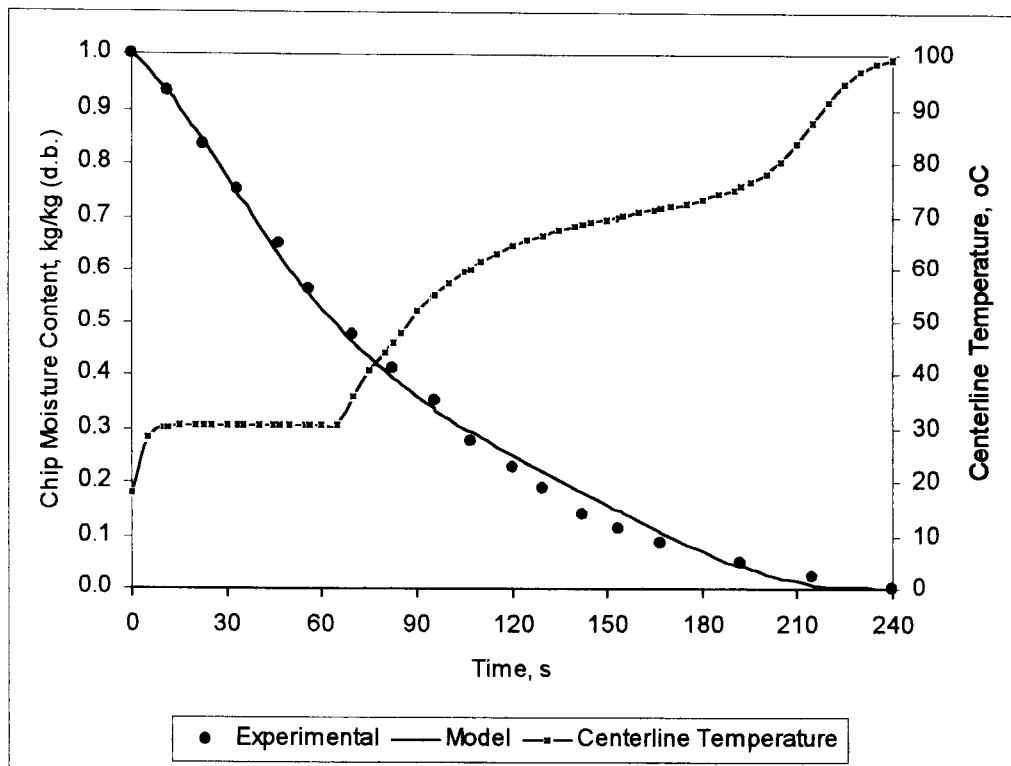


FIG. 2. Comparison of experimental and model results for chip moisture at an air temperature of 100°C and a relative humidity of 1.8%, and simulated temperature at chip centerline.

into (N+1) control volumes. The implicit finite volumes method (Patankar 1986) was used. The system was solved and converged by the TDMA line by line method.

The equilibrium correlations, Eqs. (4) and (5), maintain differential partial Eqs. (1), (2), and (3) coupled; so the algorithm developed solves the basic equations and equilibrium correlations separately at each time increment, thus preserving the simultaneity of the solution.

The basic steps of the algorithm are as follows:

- 1) The initial values of variables and constants are given. The time and space increments are set up.
- 2) The physical and transport properties are set up for each nodal point.
- 3) The algebraic transport equations for heat and liquid are solved.
- 4) The equilibrium equations are solved.
- 5) The calculated and admitted concentration and temperature profiles are compared, if the difference is less than a given error the calculation follows up. The error limit adopted was 0.1%.
- 6) The results are recorded.
- 7) The time is increased, a new step is commenced.

The calculation finishes when a previously fixed final mean moisture content, is reached.

#### RESULTS

The experimental results of Kayihan (1982), for chips of *Pinus virginiana*, were compared with the model developed, to verify their agreement and determine the constants of the transport mechanisms adopted.

In Fig. 2 the simulation results for air as the

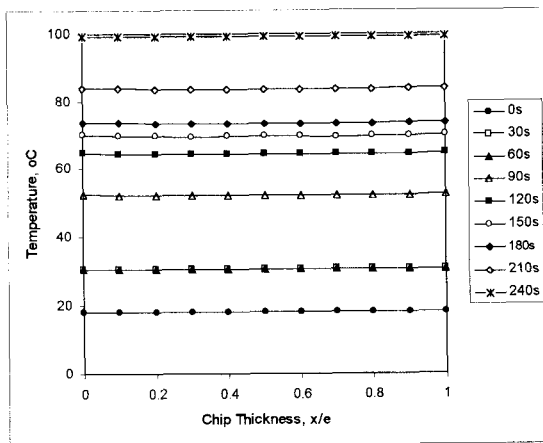


FIG. 3. Temperature profiles of *Pinus virginiana* chips through time, at a drying air temperature of 100°C and a humidity of 1.8%.

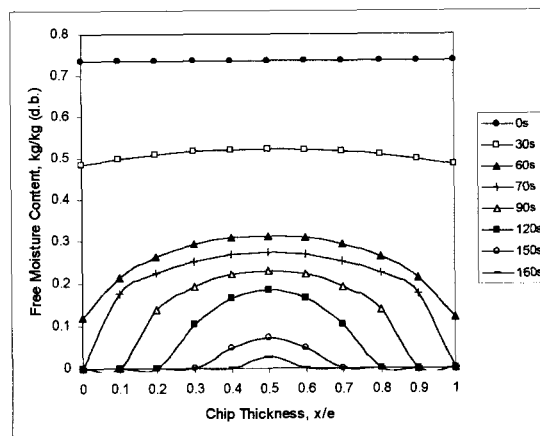


FIG. 4. Profiles of free water concentration of *Pinus virginiana* chips through time, at a drying air temperature of 100°C and a humidity of 1.8%.

dry agent at 100°C and a relative moisture content of 1.8% are shown. Porosity of the dry *Pinus virginiana*, is,  $\epsilon_s = 0.73$ , and the chip dimensions are  $0.49 \times 9 \times 46$  mm.

The best values for the constants obtained in this case were

$$k\phi = 3.0 \times 10^{-15} \text{ m}^2,$$

$$D_b^* = 1.0 \times 10^{-13} \text{ kg/m}^3 \text{ s}; \quad S_{ir} = 0.1,$$

$$\alpha = 0.004; \quad h_m = 29 \text{ J/m}^2 \text{ sK}$$

Figure 2 shows a good agreement between the experimental and simulated results for wood moisture content.

Moreover, in Fig. 2 the modeled center temperature is shown. It remains constant for an initial period of 65 s, which corresponds to the constant drying rate period, and then begins to increase slowly until reaching air temperature at the end of drying.

Figure 3 shows the temperature profiles by chip thickness, which are constant at every instant during the process; this means that the thermal conductivity of the wood is high enough to permit the free transfer of heat from the surface to inside of the chip, so it does not act as a limiting factor.

Figures 4, 5, and 6 show the concentration profiles of each of the phases considered in the

drying process: free water, bound water, and vapor.

Figure 4 shows that, for a time of 70 s, the chip surface has no more free water and an evaporation front appears, limiting the region where free water still exists. The pathway of this front by thickness can be seen: at 70 s, it is near by the surface, at 90 s, it is at 0.1 x/e; at 120 s, it is at 0.2; and at 150 s, it is at 0.3 x/e. The process finishes at 170 s, when no more free water exists inside the chip.

Figure 5 shows that the concentration pro-

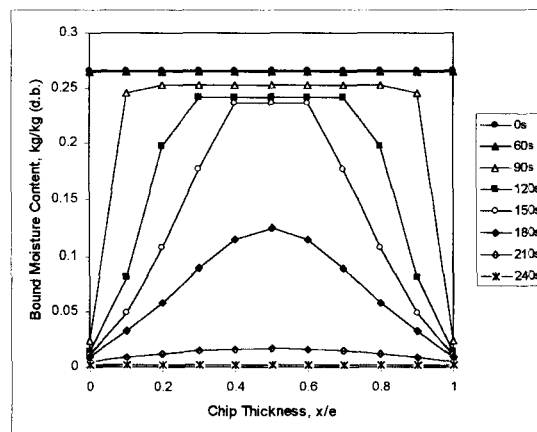


FIG. 5. Profiles of bound water concentration of *Pinus virginiana* chips through time, at a drying air temperature of 100°C and a humidity of 1.8%.

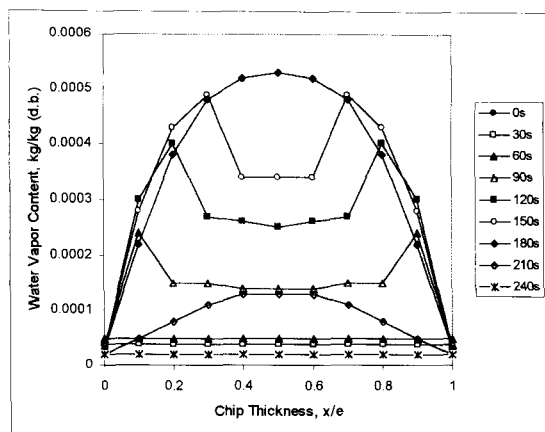


FIG. 6. Profiles of water vapor concentration in *Pinus virginiana* chips through time, at a drying air temperature of 100°C and a humidity of 1.8%.

files of bound water remain constant while free water is present. This phenomenon occurs because the bound water remains in equilibrium with the saturated vapor, and it changes (slowly) only as the temperature changes. The rate of transfer of bound water is important only away from the region limited by the evaporation front. Beginning the moment this front disappears, concentration and rate of transfer of bound water between the center and the surface diminish to the end of the drying process.

The profiles of vapor concentration inside the chip are presented in Fig. 6. They follow the free water profiles, so the concentration is low and nearly constant at the beginning (see the profiles for 0, 30, and 60 s). Vapor at these conditions is saturated, and its concentration inside this porous medium depends only on temperature and wood porosity. The profiles change slightly from one thickness point to another due to the increase in effective porosity as the free water inside the wood decreases.

From 70 s, the profiles follow the bound water profiles at the outer part of the chips, where vapor concentration is given by the sorption isotherms of wood; in the inner part, vapor concentration still depends on temperature, which increases slowly. The differentials of concentration between inside and out-

side are increasing at the same time that the evaporation front moves towards the center. This feature continues up to 180 s, when vapor concentration reaches its maximum value (the evaporation front disappears) and begins a decrease that continues to the end of the process.

#### *Order of magnitude of the different effects in the mass and energy conservation equations*

The order of magnitude of the different effects present in the mass and energy conservation equations are discussed in this section. The aim is to validate the factors considered (and disregarded) in the model presented in this work.

From the mass conservation equation for water (1), we have the liquid diffusion effect,  $DJ_{bf}$ , as follows:

$$DJ_{bf} = -\frac{\partial J_{bf}}{\partial x}$$

and the evaporation/condensation effect, which is the evaporative ratio,  $EE_{vbf}$ :

$$EE_{vbf} = -R_{evap}$$

The values of these effects as a function of time are presented in Fig. 7. These values were obtained from the simulation proposed here for wood chips of *Pinus virginiana*, for which experimental data compared with the kinetic model are presented in Fig. 2. The values are relative to the surface and level 0.2 inside the chip; to facilitate the reading, absolute values are presented on a logarithmic scale.

In Fig. 7 it can be observed that the effects of diffusion and condensation/evaporation on the surface of the chip are of the same order of magnitude. For level 0.2, the order of magnitude of the first relative to the second is very variable. For a time of 15 s, the diffusion effect is ten thousand times greater than that of evaporation/condensation; but for the period of 120 to 180 s, it is between five and ten times lower. The condensation/evaporation effect becomes greater than the diffusion effect, for level 0.2 inside the chip, as soon as the

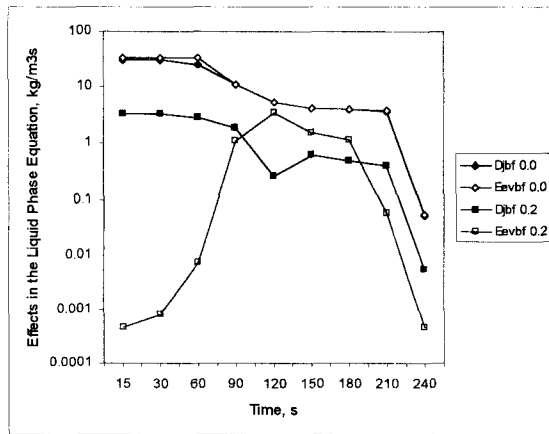


FIG. 7. Effects of the diverse mechanisms of mass transfer in the mass conservation equation as a function of time, on the surface and at level 0.2 in the wood chip. DJbf: mass diffusion, liquid phase; Eevbf: effect of condensation/evaporation at the surface of the chip; wood: *Pinus virginiana*; drying agent: air at 100°C and 1.8% relative humidity.

evaporation front reaches this level (see Fig. 4). The condensation/evaporation effect remains greater than the diffusion effect up to the moment that the evaporation front disappears (at this moment, there is no longer any free water inside the chip). Beginning at this moment, it decays abruptly and remains lower than the diffusion effect. This behavior remains the same for other levels inside the chip.

The complete equation of energy conservation is

$$(\rho_{sw}c_{psw})\frac{\partial T}{\partial t} = -\frac{\partial J_q}{\partial x} - \Delta HR_{evap} - J_{bf}c_{pbf}\frac{\partial T}{\partial x} - J_v c_{pv}\frac{\partial T}{\partial x}$$

The heat conduction effect, DJq, is

$$DJq = -\frac{1}{(\rho_{sw}c_{psw})}\frac{\partial J_q}{\partial x}$$

The evaporation/condensation effect, EEV, is

$$EEV = -\frac{\Delta HR_{evap}}{(\rho_{sw}c_{psw})}$$

The effect of heat convection due to the diffusion of liquid, ECBf, is

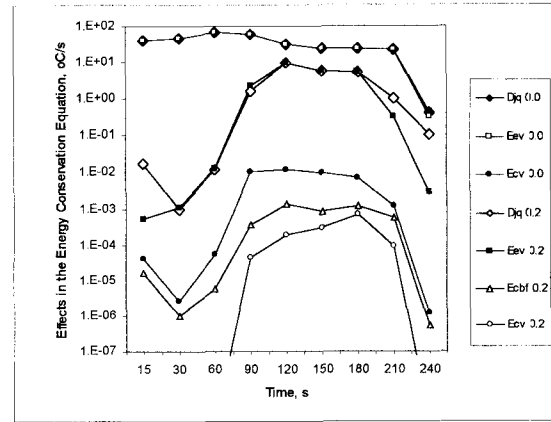


FIG. 8. Effects of the diverse mechanisms of heat and mass transfer in the energy conservation equation as a function of time, on the surface and at level 0.2 in the wood chip. DJq: heat conduction; EEv: effect of condensation/evaporation; ECv: convection by diffusion of liquid; ECBf: effect of convection due to liquid diffusion; wood: *Pinus virginiana*; drying agent: air at 100°C and 1.8% relative humidity.

$$ECbf = -\frac{J_{bf}c_{pbf}}{(\rho_{sw}c_{psw})}\frac{\partial T}{\partial x}$$

The effect of heat convection due to the diffusion of water vapor, ECv, is

$$ECv = -\frac{J_v c_{pv}}{(\rho_{sw}c_{psw})}\frac{\partial T}{\partial x}$$

The values of these effects are shown in Fig. 8. As in the previous case, they were obtained from the simulation proposed here for wood chips of *Pinus virginiana*, for which experimental data compared with the kinetic model are presented in Fig. 2.

In Fig. 8 it can be observed that on the surface of the chip, the effects of conduction and evaporation/condensation are of the same order of magnitude for any time; but the effect of heat convection due to the diffusion of vapor is, practically the entire time, one thousand times lower than the other two. The effect of heat convection at the surface by liquid diffusion is null, due to the fact that the flux of liquid from the surface to the external boundary layer is also null. Because of that, this effect does not appear in Fig. 8.

For level 0.2 inside the chip, the conduction effect varies from ten times higher to the same order of magnitude as the evaporation effect, but the effect of convection of liquid is ten thousand times lower than the other two; and the effect of convection of vapor is one hundred thousand times lower, when it does exist. This behavior remains the same for other levels inside the chip.

These observations show that the effects of heat convection due to the diffusion of vapor and liquid can be disregarded in the equation of energy conservation, as was done in the model presented in this work, for a temperature level of 100°C in the air as drying agent. However, as the condensation/evaporation effect, coupled to heat and mass transfer, is present during the entire drying time and is of the same order of magnitude as the conduction effect at any point inside the chip, it can not be disregarded under the same conditions of the drying agent.

It can be observed that the effect of evaporation/condensation at the surface decays in absolute value from the moment that the free water has totally disappeared at the surface (70 s), the reason being that vapor pressure at the surface no longer corresponds to saturation and that the evaporation rate,  $R_{\text{evap}}$ , diminishes. This produces an increase in chip temperature. The temperature differential in the external boundary layer decays, producing the decrease in the heat flow rate from air to chip. The effect of heat conduction at the surface also diminishes.

Relative to the level 0.2, the evaporation effect begins to increase from the moment that the free liquid water starts to migrate from the pores in the wood and the vapor begins to occupy these spaces. The order of magnitude of conduction and evaporation effects remains the same as long as the evaporation front is still present, but there is no longer any free water inside the chip. These two effects continue to increase until the instant that the drying front reaches that level. Beginning at this moment, the evaporation/condensation effect

decays at the same magnitude as the conduction effect.

These observations confirm what was said before about the evaporation/condensation effect: it can not be disregarded for the temperature level of 100°C in air, as drying agent at 1.8% moisture content.

#### CONCLUSIONS

A model was presented for the drying of wood chips, which considers the most important mechanisms of heat and mass transfer inside the solid. The results of the numerical simulation were compared with experimental data from the literature, showing a good agreement.

Results on the effect of each of the mechanisms of heat and mass transfer were shown and discussed, justifying the terms disregarded in the model. Thus the transport mechanisms considered, capillarity of free water, diffusion of vapor and bound water, and heat conduction also with evaporation/condensation inside the chips, were adequate to describe the phenomena for air and *Pinus* wood chips under the conditions tested.

The program developed could be used to simulate the one-dimensional drying of other porous hygroscopic capillary means. To do so, basic information about the solid is necessary, i.e., data on the drying total kinetics and isotherms of equilibrium. The program could be extended to the two or three-dimensional cases.

#### NOTATIONS

##### Latin letters

b	Chip length	M
C	Concentration	Kg/kg (d.b.)
$c_p$	Specific heat	J/kg K
$\bar{c}_p$	Molar specific heat	J/mol K
D	Diffusivity	$\text{m}^2/\text{s}$
$D_b^*$	Constant of bound water diffusivity	$\text{kg}/\text{s m}^3$
DJq	Conductive effect in the energy conservation equation	$^\circ\text{C}/\text{s}$
DJbf	Diffusivity effect in the mass (liquid) conservation equation	$\text{kg}/\text{s m}^3$
e	Chip thickness	M
ECbf	Heat convective effect due to liquid diffusion in the energy conservation equation	$^\circ\text{C}/\text{s}$

ECv	Heat convective effect due to vapor diffusion in the energy conservation equation	$^{\circ}\text{C/s}$
EEv	Condensation/evaporation effect in the energy conservation equation	$^{\circ}\text{C/s}$
EEvbf	Condensation/evaporation effect in the mass (liquid) conservation equation	$\text{kg/s m}^3$
$h_m$	Heat transfer coefficient between external air and the free surface of porous medium	$\text{J/m}^2 \text{ s K}$
J	Mass flux	$\text{kg/s m}^2$
$J_q$	Conduction heat transfer flux	$\text{J/s m}^2$
K	Heat conductivity of humid solid	$\text{J/m s K}$
$k_r$	Permeability of solid to free water	$\text{m}^2$
$k_r^{\phi}$	Constant for permeability of solid to free water	$\text{m}^2$
$k_m$	Mass transfer coefficient	$\text{kg/m}^2 \text{ s Pa}$
L	Chip width	m
$M_v$	Water vapor molecular mass	$\text{kg/mol}$
P	Total gas pressure	Pa
$P_c$	Capillary pressure	Pa
Pr	Prandtl number	
$p_v$	Partial pressure of water vapor inside the solid	Pa
R	Universal constant of gases	$\text{J/mol K}$
$R_{\text{evap}}$	Evaporation rate of liquid in the solid	$\text{kg/m}^3 \text{ s}$
Sc	Schmidt number, for the external air	
$S_r$	Irreducible saturation	
$S_v$	Entropy of water vapor	$\text{J/mol K}$
T	Temperature of solid	K
t	Time	S
X	Moisture content of solid (d.b.)	$\text{kg/kg (d.b.)}$
x	Spatial variable	m

#### Initial Greek letters

$\alpha$	Obstruction factor of pores in wood	
$\Delta H$	Vaporization enthalpy	$\text{J/kg}$
$\epsilon$	Effective fractional void space	
$\epsilon_s$	Fractional void space of the dry solid	
$\eta$	Dynamic viscosity	$\text{kg/m s}$
$\mu$	Chemical potential	$\text{J/kg}$
$\rho$	Density	$\text{kg/m}^3$

#### Subscripts/superscripts

a	Air
a,v	Vapor in air (diffusivity)
b	Bound water
bf	Liquid water
f	Free water
fbp	Fiber saturation point
g	External humid air
rp	Random diffusivity of air in a porous medium
s	Dry solid
sat	Saturation point

sw	Wet solid
v	Water vapor
o	Chip surface

#### ACKNOWLEDGMENTS

The authors are indebted to their friend and colleague, Clayton Dimas Ribeiro Fernandes at the Instituto de Pesquisas Tecnológicas, S.P., Brazil, for his invaluable help in the computational work.

The authors would like to express their gratitude to the Conselho Nacional de Desenvolvimento Científico e Tecnológico (CNPq) for its financial support.

#### REFERENCES

- BIRD, R. B., W. E. STEWART, AND E. N. LIGHTFOOT. 1960. Transport phenomena. John Wiley & Sons, New York, NY. 780 pp.
- KANURY, A. M. 1975. Introduction to combustion phenomena. Gordon and Breach, New York, NY. (citation only).
- KAYIHAN, F. 1982. Simultaneous heat and mass transfer with local three-phase equilibrium in wood drying. In J. C. Ashworth, ed. Proc. 3rd International Drying Symposium, Birmingham, England.
- PATANKAR, S. 1986. Numerical heat transfer and fluid flow. Hemisphere Publishing, New York, NY. 192 pp.
- SIMPSON, W. T., AND H. N. ROSEN. 1981. Equilibrium moisture content of wood at high temperatures. Wood Fiber 13(3):150–158.
- SIAU, J. F. 1971. Flow in wood. Syracuse University Press, Syracuse, NY. (citation only).
- SOUZA, M. E. P. 1994. Transporte de massa e calor na secagem de cavaco de madeira. Campinas. Master thesis, Universidade Estadual de Campinas, Faculdade de Engenharia Mecânica, São Paulo, Brazil. 102 pp.
- SPOLEK, G. A., AND O. A. PLUMB. 1981. Capillary pressure in softwoods. Wood Sci. Technol. 15:189, (citation only).
- STANISH, M. A., G. S. SCHAJER, AND F. KAYIHAN. 1986. A mathematical model of drying for hygroscopic porous media. AiCHE J. 32(8):1301–1311.
- TESORO ET AL. 1974. Relative permeability and the gross pore structure of wood. Wood Fiber 6(3):226, (citation only).
- WEAST, R. C. 1974. Handbook of Chemistry and Physics. 56th. ed. CRC Press, Cleveland, OH. P. F49, (citation only).
- WOOD HANDBOOK. 1974. Wood as an engineering material. USDA Forest Serv. Forest Prod. Lab., Madison, WI (citation only).